

**APPENDIX B. WAVE TRANSFORMATION NUMERICAL MODELING
INFORMATION**

B1. Directional and Frequency Verification

Presented in this appendix are seasonally-based directional and frequency spectral plots at WIS stations 1046 and 1047 (Figures B1-1 through B1-8). These figures illustrate the seasonal input conditions used at Grid A (WIS 1047 data) and Grid B (WIS 1046 data). The WIS data are plotted as histogram plots, and the generated spectra are represented by solid black lines. Each figure includes directional verification and utilization, as well as frequency verification and utilization.

The generated spectra (direction and frequency) are tailored to reflect the associated wave climate during each season at each site. This is accomplished by a combination of techniques. It includes:

- determining seasonal wave statistics at each site
- stretching or compressing the directional or frequency spread

Both of these allow a custom fit of WIS wave data to generated spectra. Sections 4.2.2.1 and 4.2.2.2 provide a more thorough discussion of directional and frequency spectral theory.

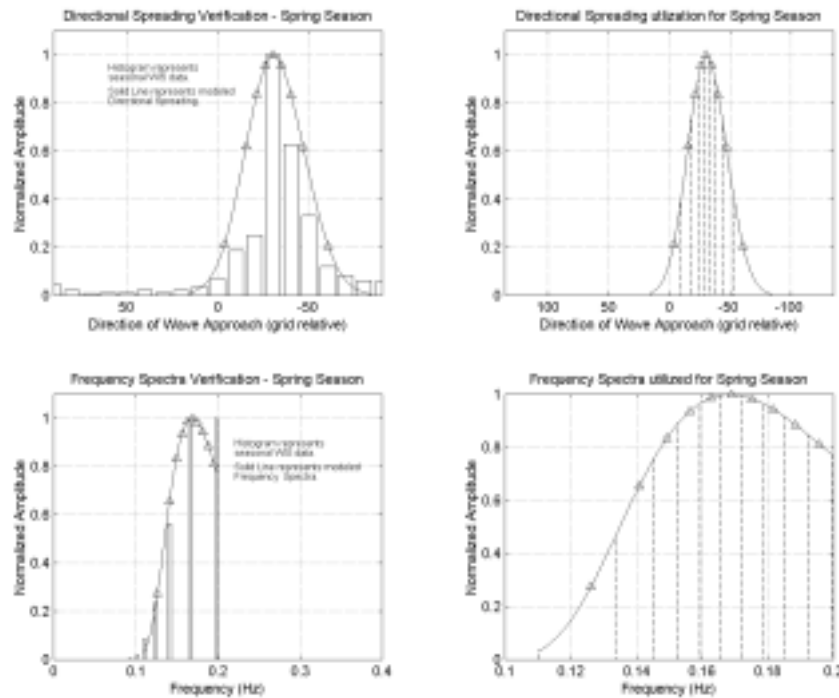


Figure B1-1. Spring spectral verification and utilization at WIS 1046.

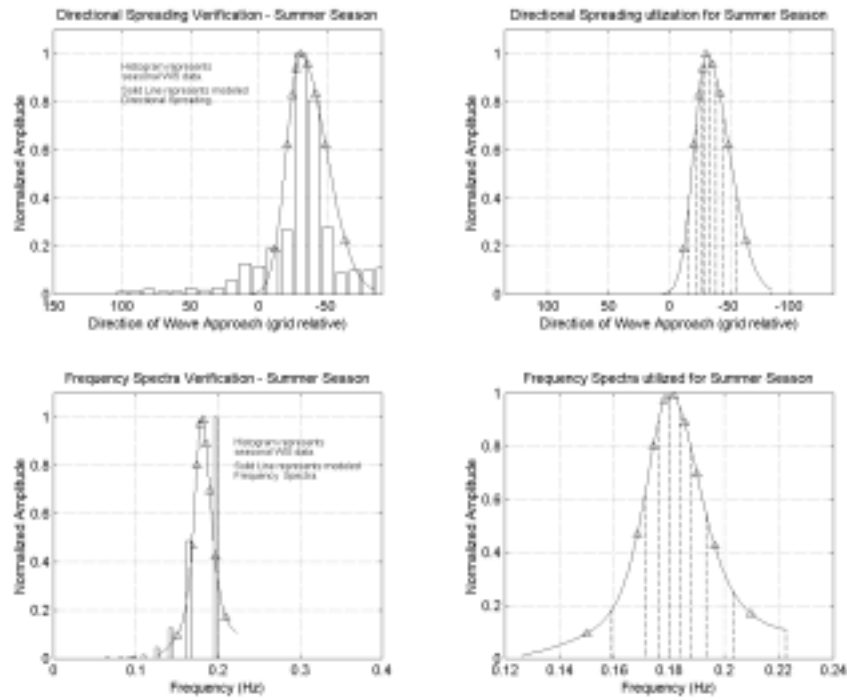


Figure B1-2. Summer spectral verification and utilization at WIS 1046.

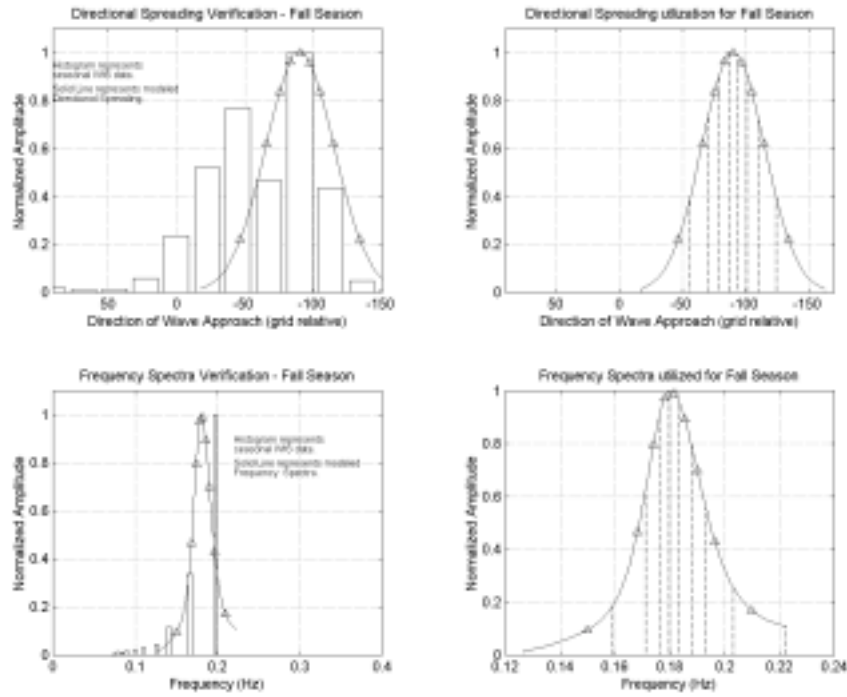


Figure B1-3. Fall spectral verification and utilization at WIS 1046.

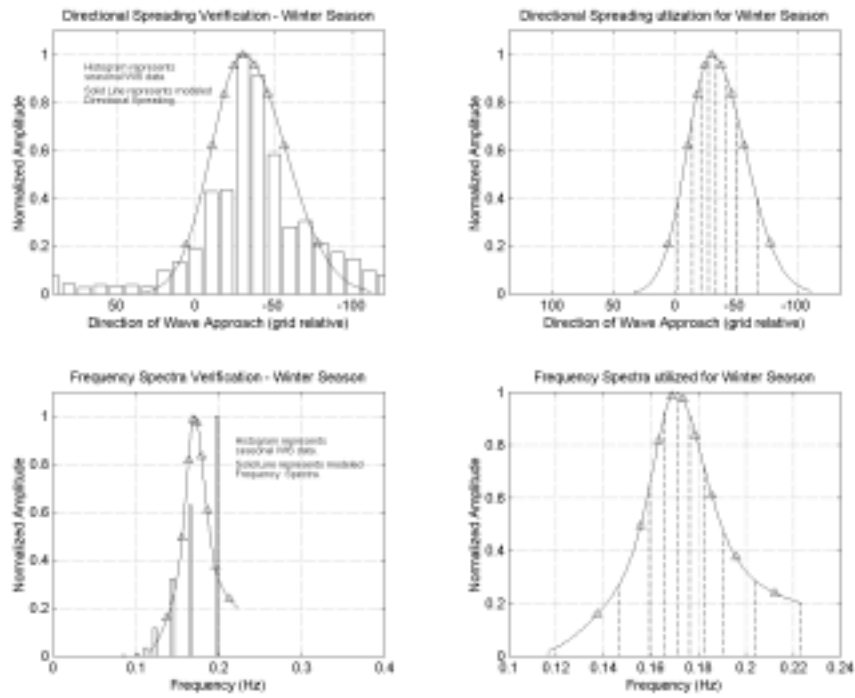


Figure B1-4. Winter spectral verification and utilization at WIS 1046.

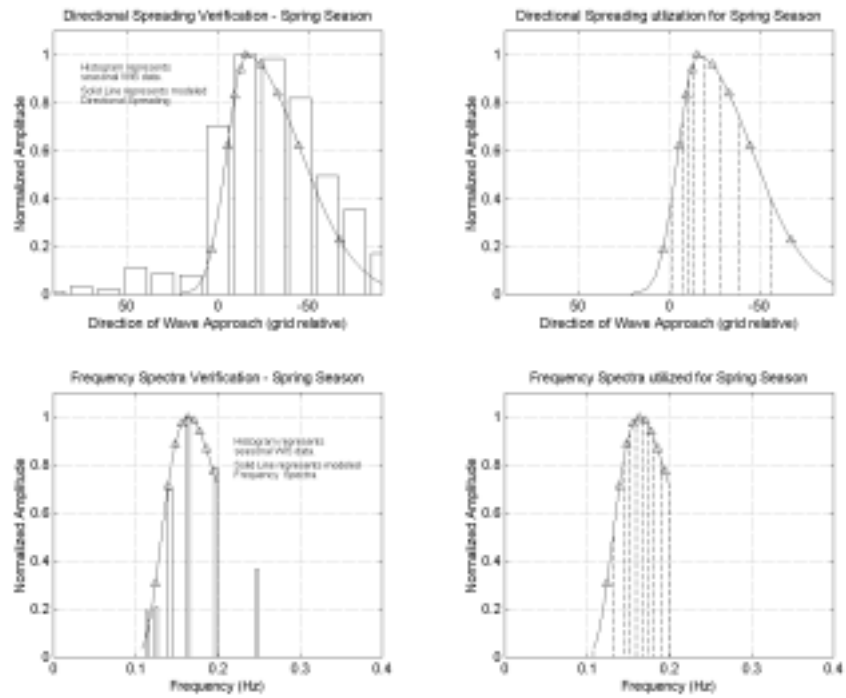


Figure B1-5. Spring spectral verification and utilization at WIS 1047.

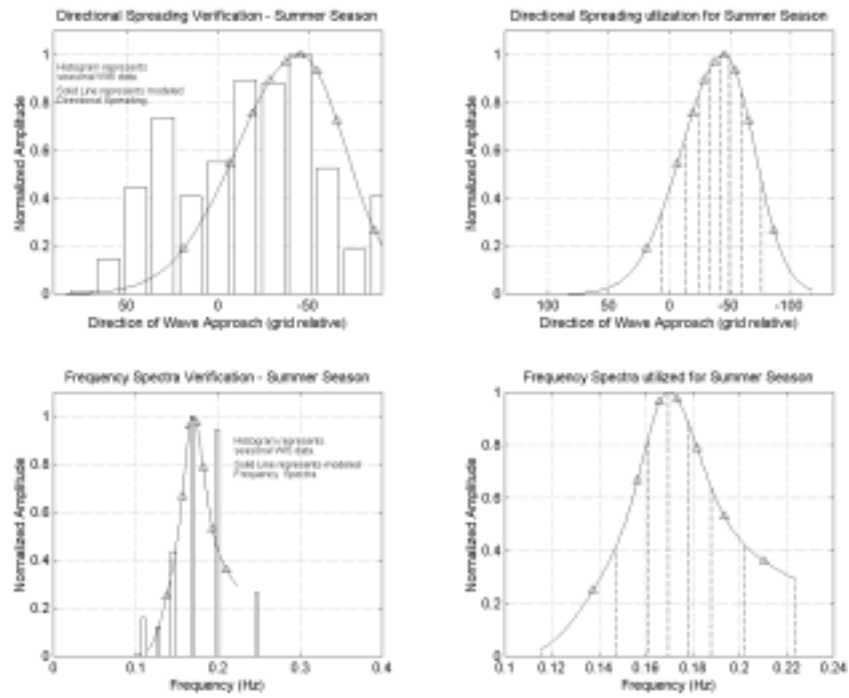


Figure B1-6. Summer spectral verification and utilization at WIS 1047.

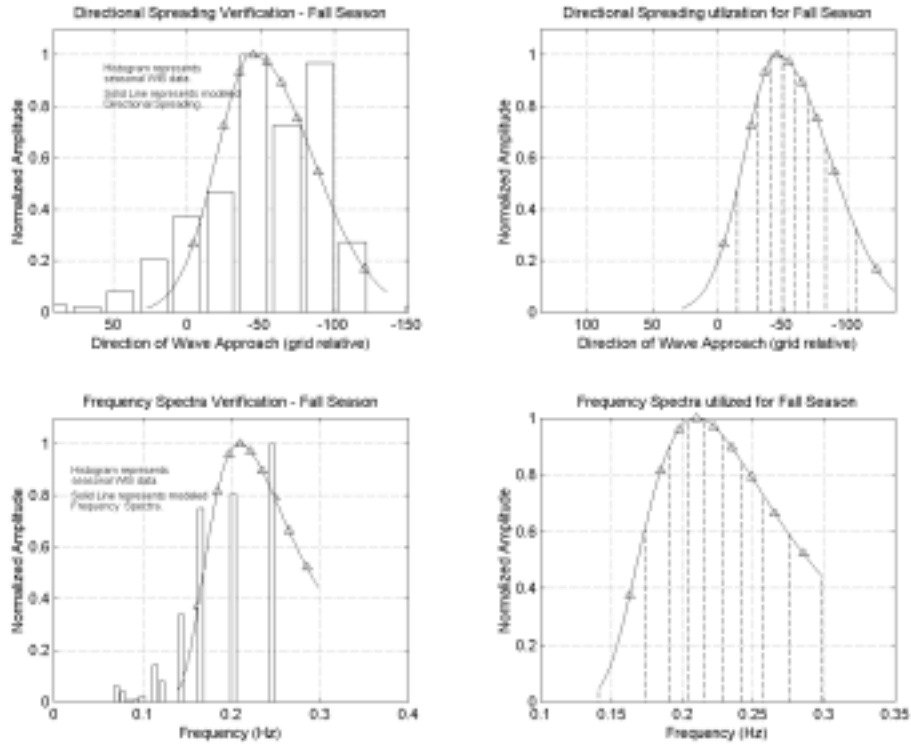


Figure B1-7. Fall spectral verification and utilization at WIS 1047.

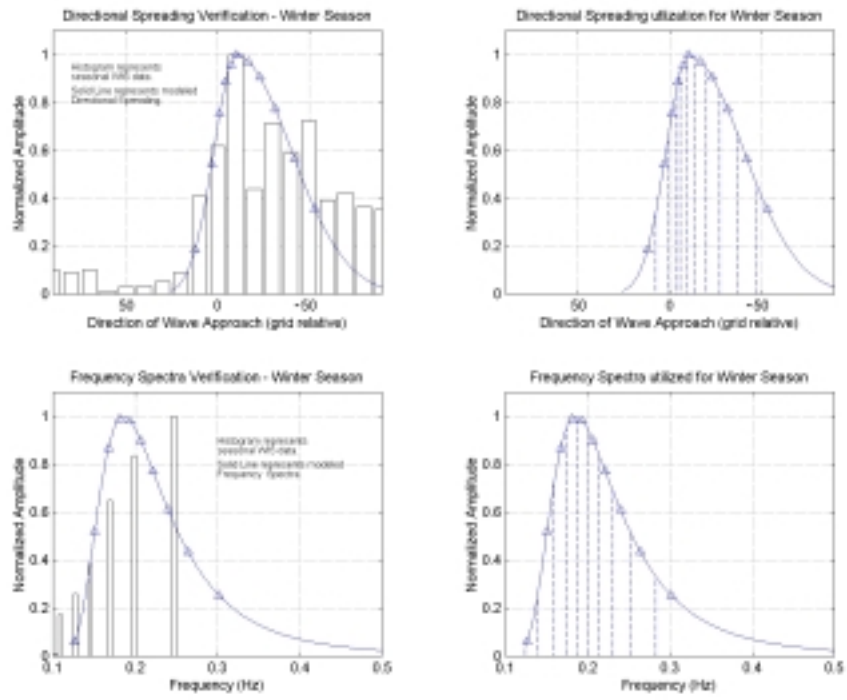


Figure B1-8. Winter spectral verification and utilization at WIS 1047.

B2. Existing Conditions Wave Model

Presented in this appendix are the existing condition (pre-dredging) numerical wave transformation modeling results. Results are presented for all of the simulations (seasonal and 50-year storm) at both grids (A and B).

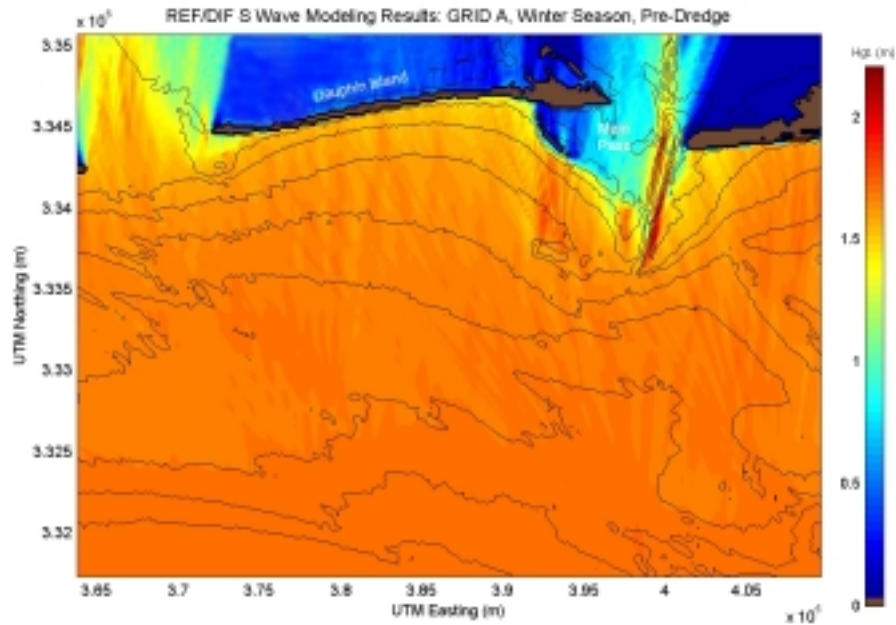


Figure B2-1. Spectral wave modeling results for existing conditions utilizing a typical winter season at reference Grid A.

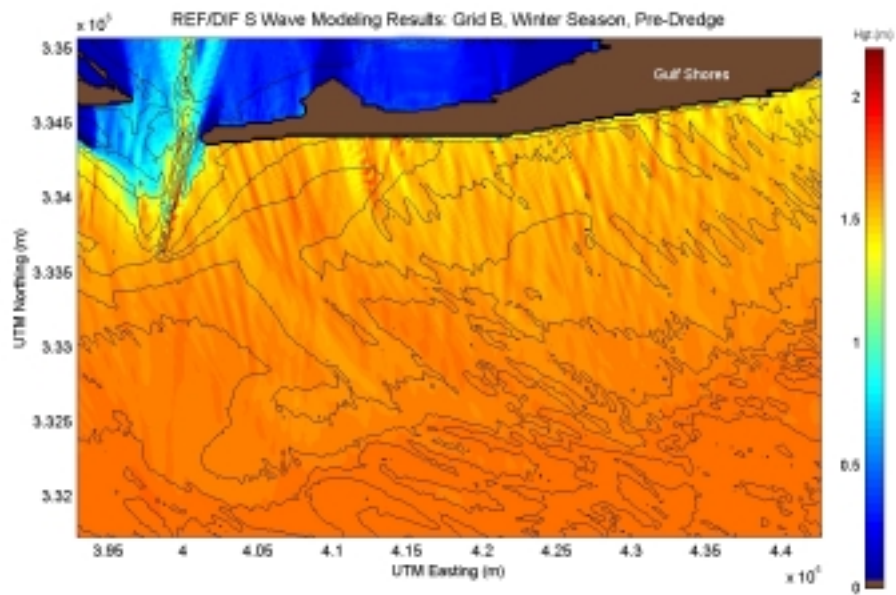


Figure B2-2. Spectral wave modeling results for existing conditions utilizing a typical winter season at reference Grid B.

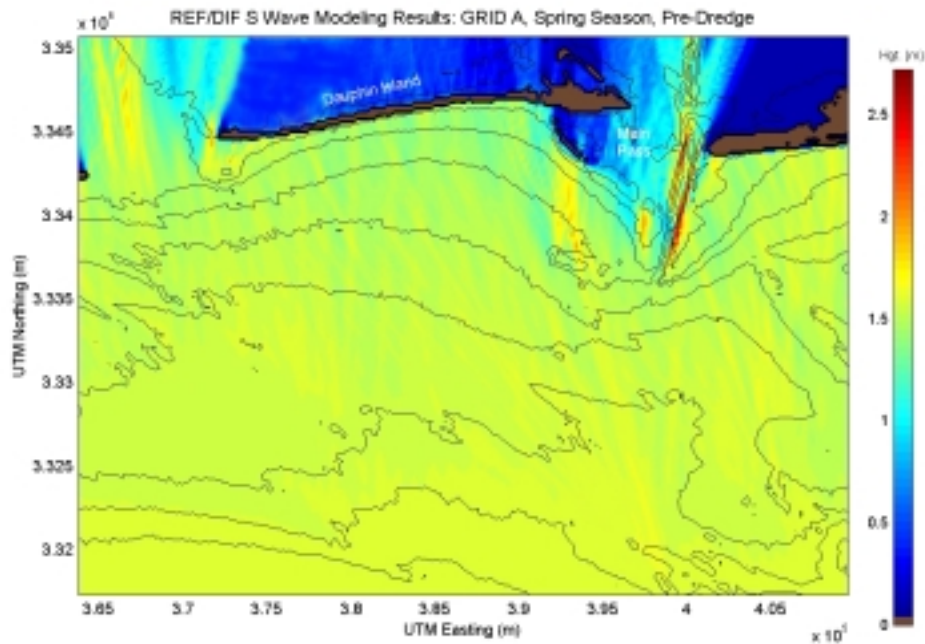


Figure B2-3. Spectral wave modeling results for existing conditions utilizing a typical spring season at reference Grid A.

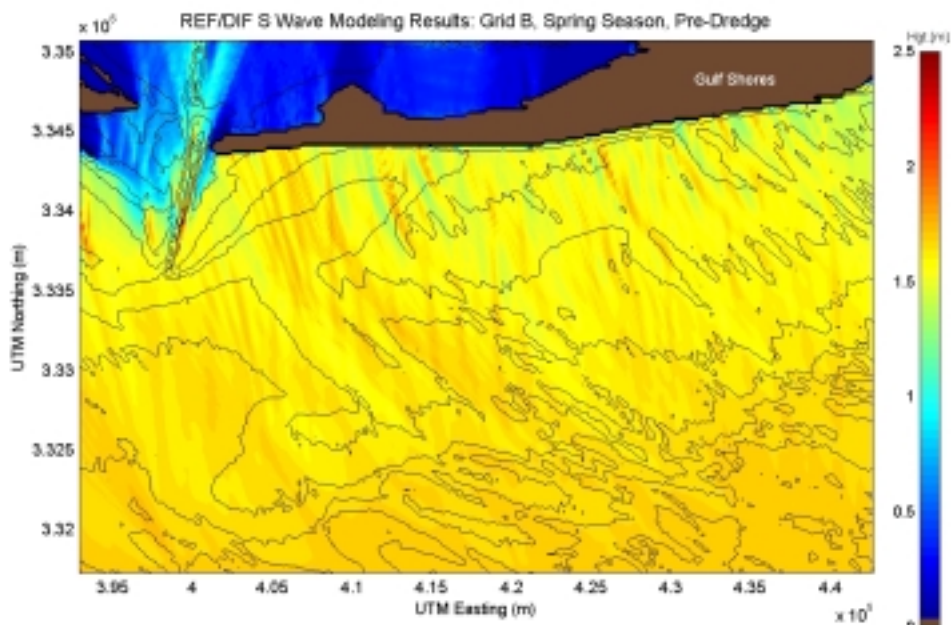


Figure B2-4. Spectral wave modeling results for existing conditions utilizing a typical spring season at reference Grid B.

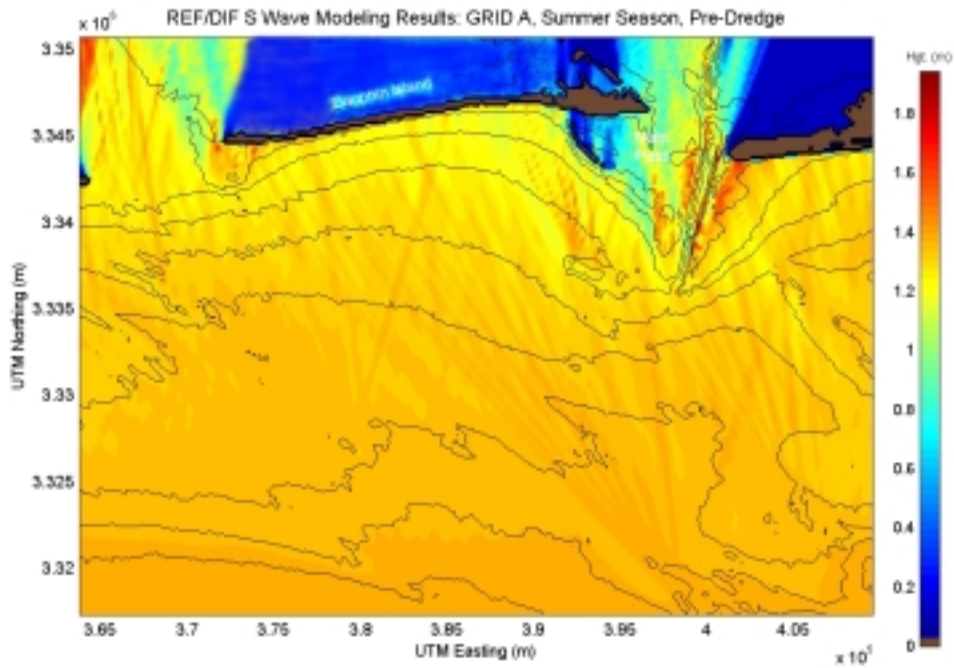


Figure B2-5. Spectral wave modeling results for existing conditions utilizing a typical summer season at reference Grid A.

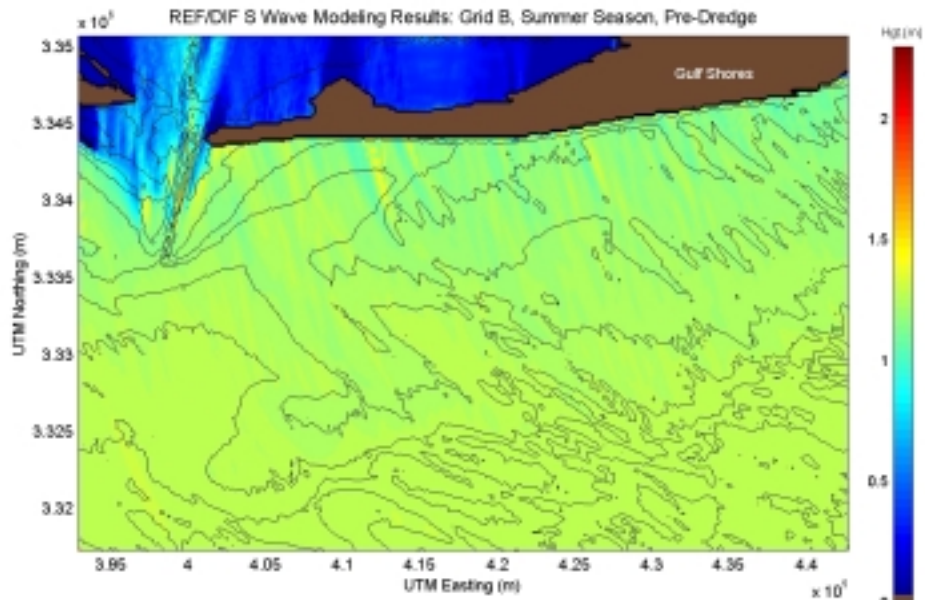


Figure B2-6. Spectral wave modeling results for existing conditions utilizing a typical summer season at reference Grid B.

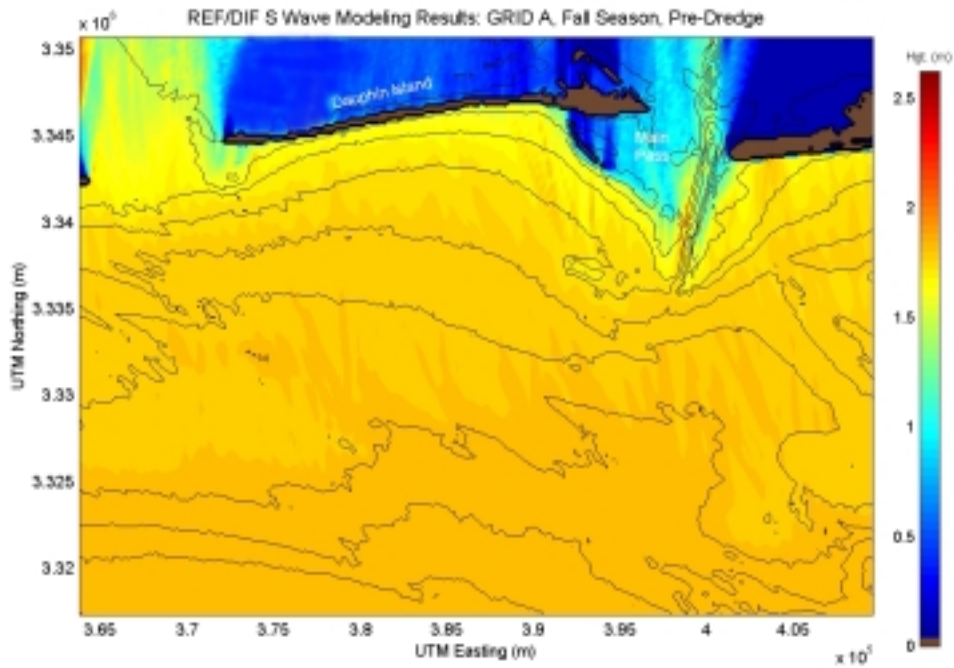


Figure B2-7. Spectral wave modeling results for existing conditions utilizing a typical fall season at reference Grid A.

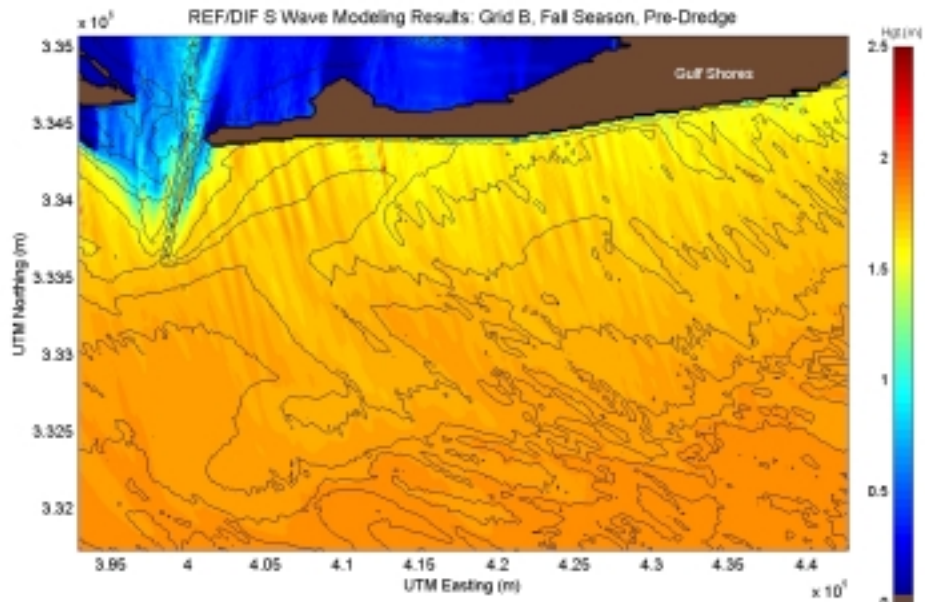


Figure B2-8. Spectral wave modeling results for existing conditions utilizing a typical fall season at reference Grid B.

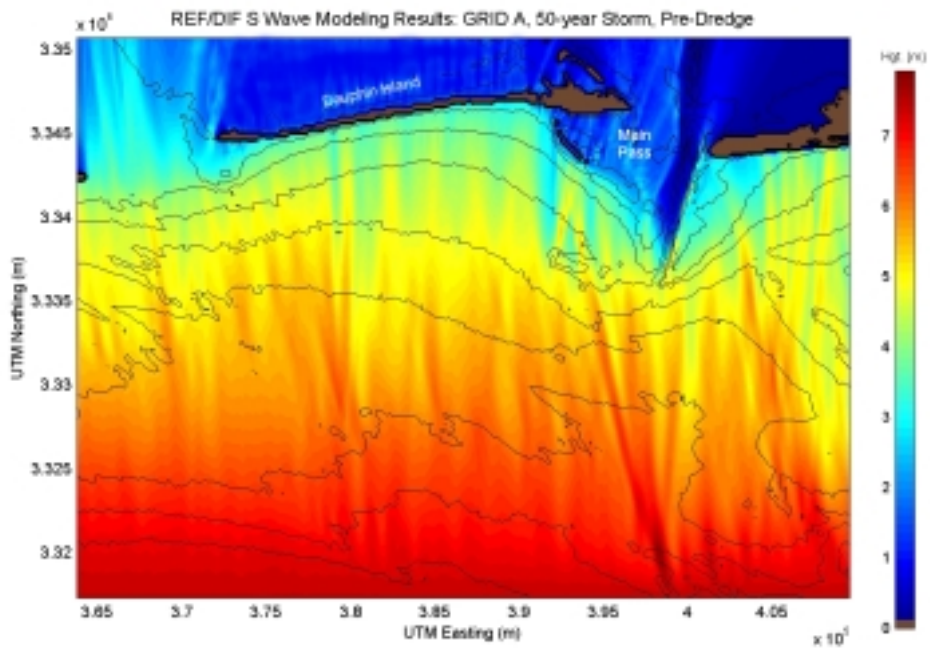


Figure B2-9. Spectral wave modeling results for existing conditions using a 50-year storm at reference Grid A.

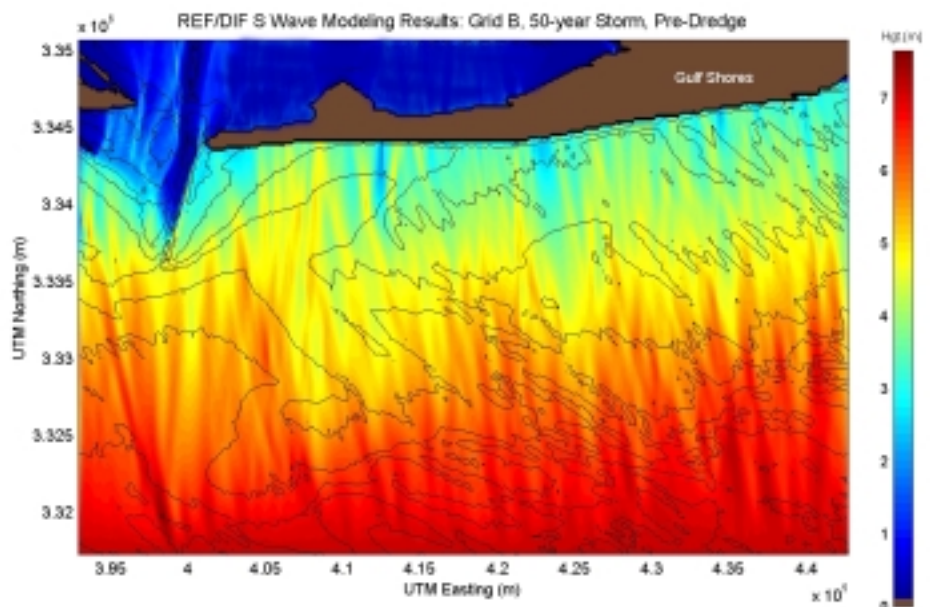


Figure B2-10. Spectral wave modeling results for existing conditions using a 50-year storm at reference Grid B.

B3. Post-Dredging Wave Model Results

Presented in this appendix are the post-dredged numerical wave transformation modeling results. Results are presented for all of the simulations (seasonal and 50-year storm) at both grids (A and B).

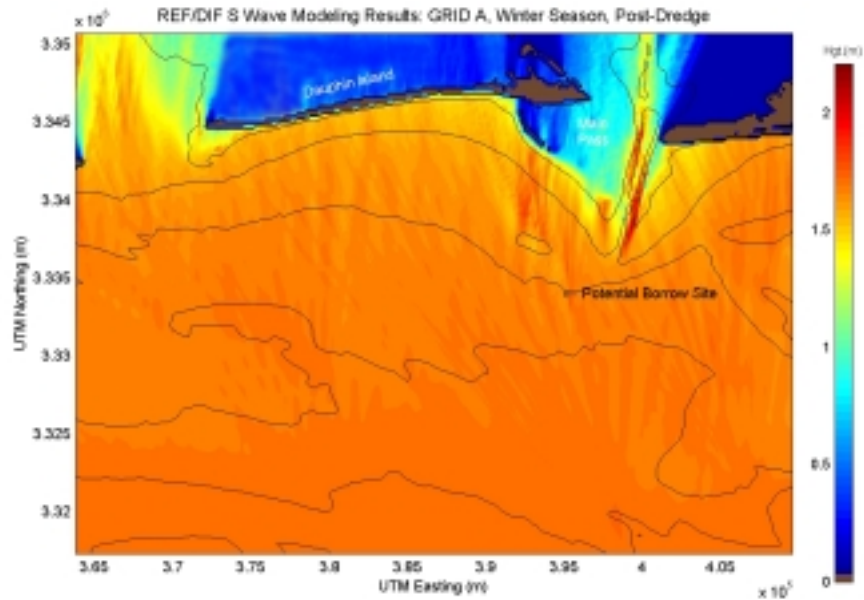


Figure B3-1. Spectral wave modeling results for post-dredged conditions utilizing a typical winter season at reference Grid A.

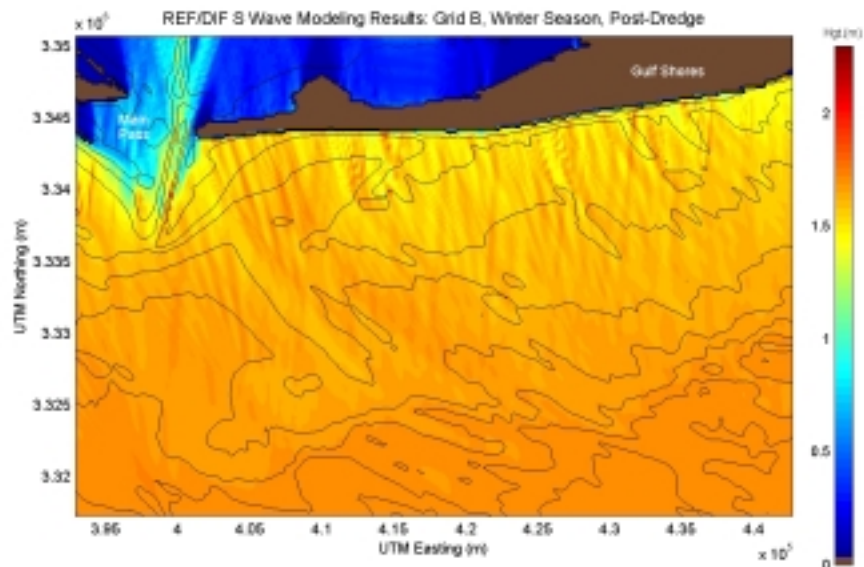


Figure B3-2. Spectral wave modeling results for post-dredged conditions utilizing a typical winter season at reference Grid B.

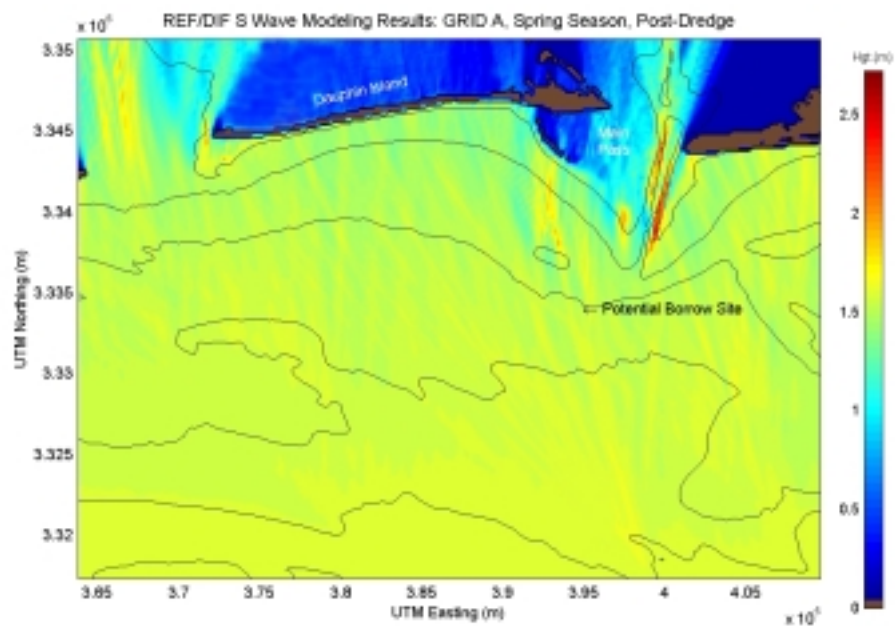


Figure B3-3. Spectral wave modeling results for post-dredged conditions utilizing a typical spring season at reference Grid A.

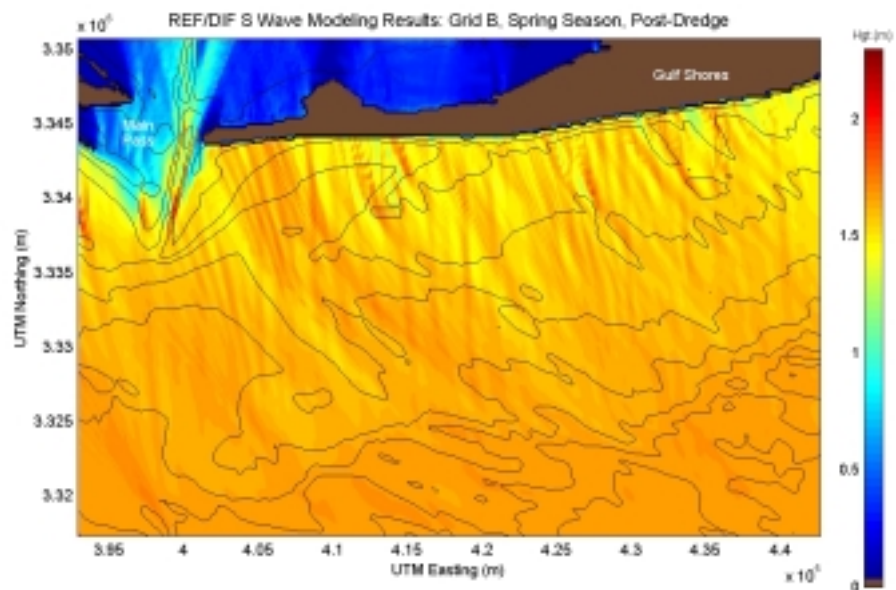


Figure B3-4. Spectral wave modeling results for post-dredged conditions utilizing a typical spring season at reference Grid B.

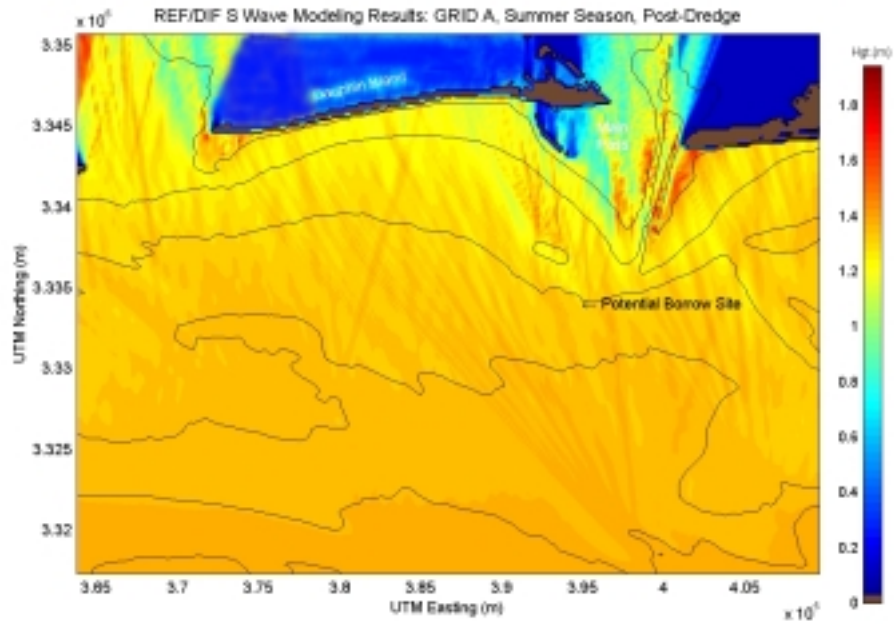


Figure B3-5. Spectral wave modeling results for post-dredged conditions utilizing a typical summer season at reference Grid A.

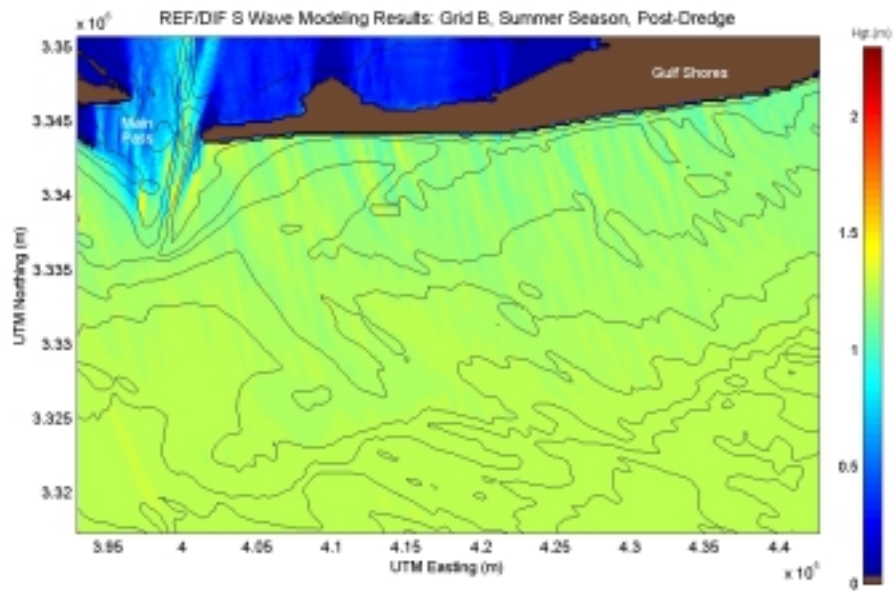


Figure B3-6. Spectral wave modeling results for post-dredged conditions utilizing a typical summer season at reference Grid B.

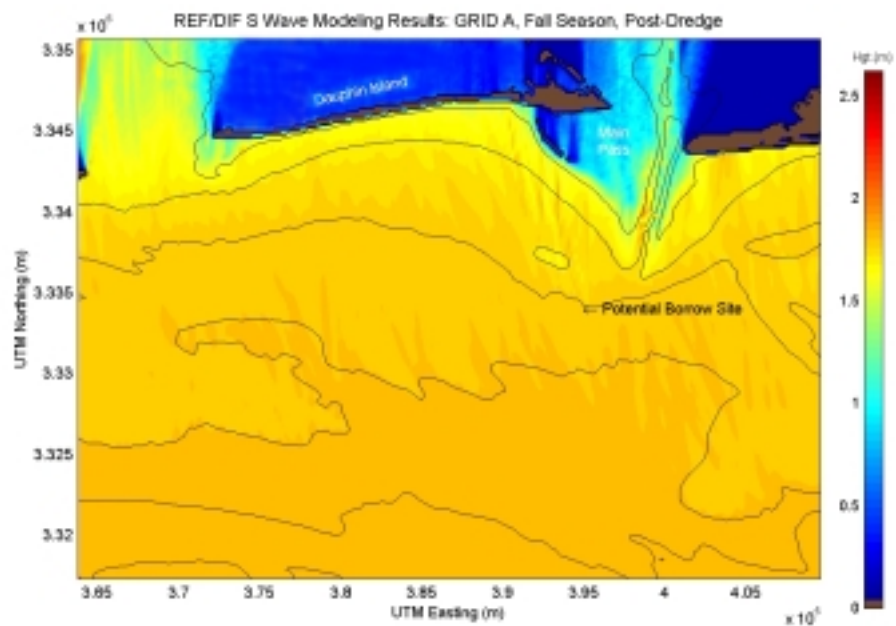


Figure B3-7. Spectral wave modeling results for post-dredged conditions utilizing a typical fall season at reference Grid A.

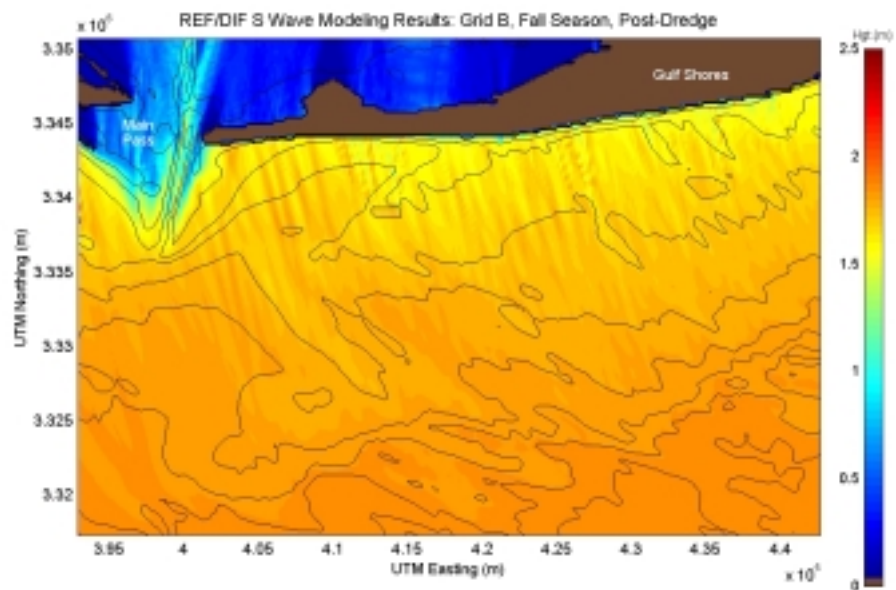


Figure B3-8. Spectral wave modeling results for post-dredged conditions utilizing a typical fall season at reference Grid B.

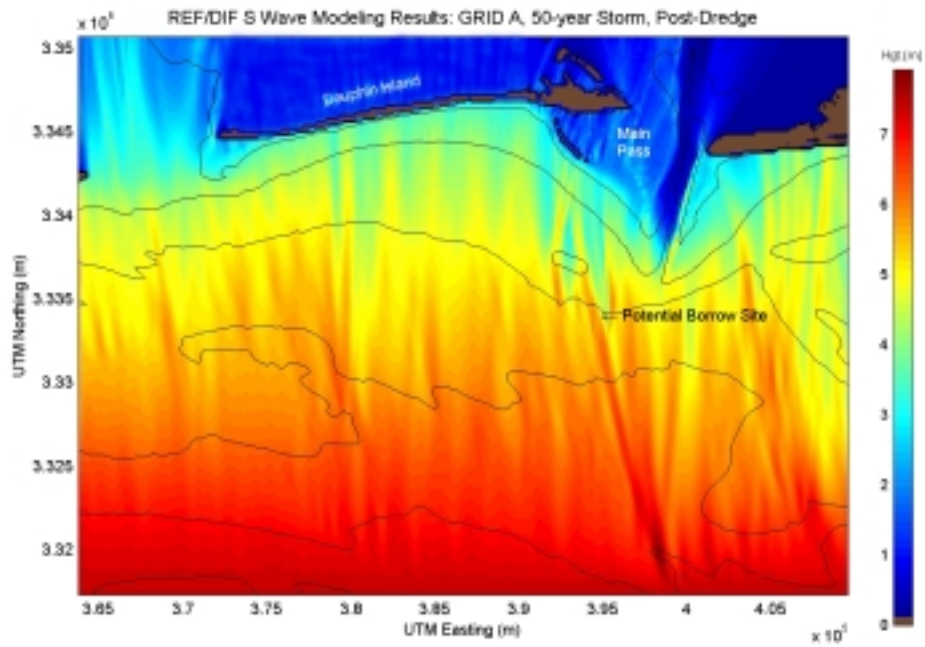


Figure B3-9. Spectral wave modeling results for post-dredged conditions utilizing a 50-year storm at reference Grid A.

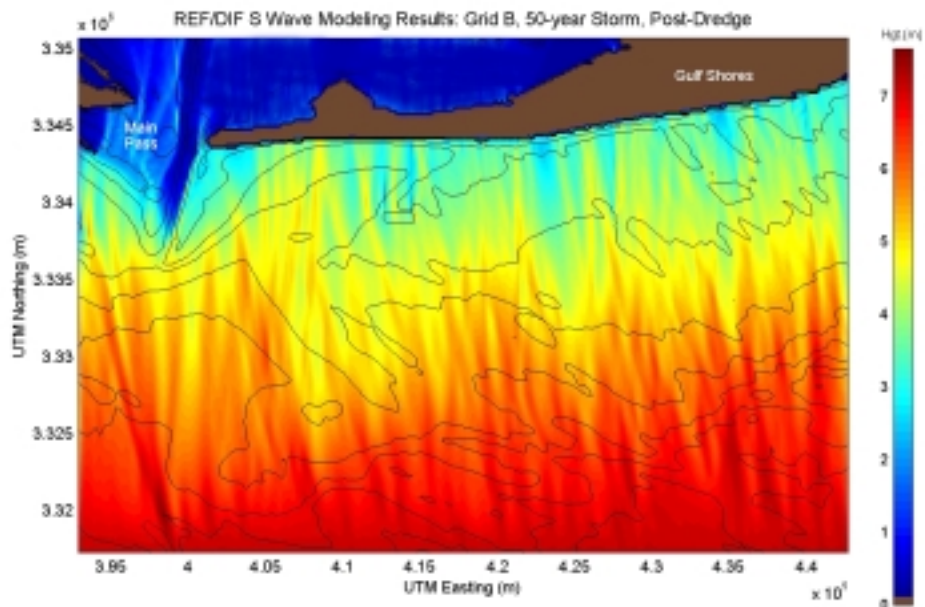


Figure B3-10. Spectral wave modeling results for post-dredged conditions utilizing a 50-year storm at reference Grid B.

B4. Pre- and Post-Dredging Difference Plots

Presented in this appendix are wave height modifications caused by the offshore sand mining of various potential borrow sites. Results are presented for all of the simulations (seasonal and 50-year storm). For all figures, hot colors (reds) identify areas of increased wave height, while cold colors (blues) identify areas of decreased wave height. Solid black lines indicate depth contours and the color bar on the right indicates the magnitude of the modifications.

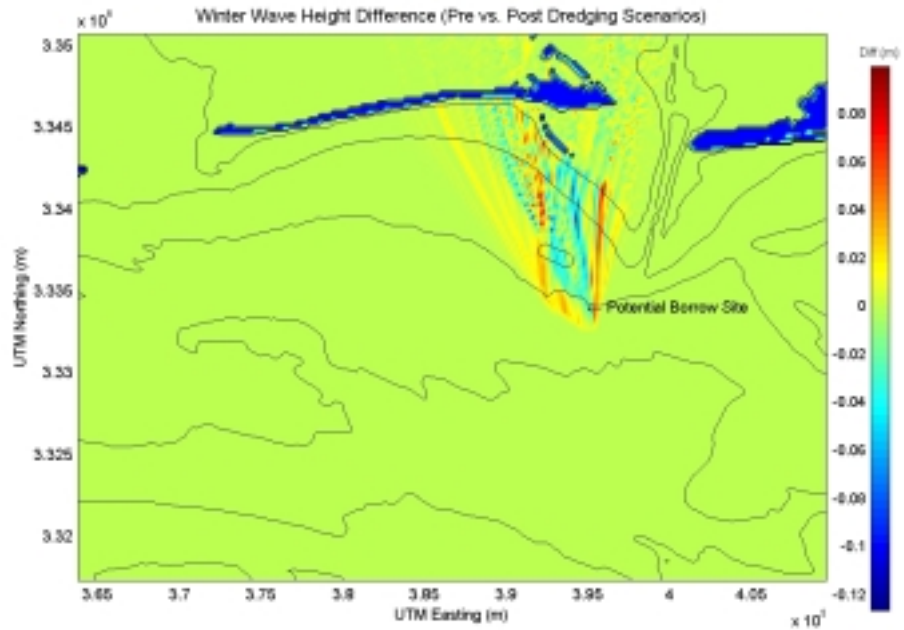


Figure B4-1. Wave height modifications caused by the offshore sand mining at Resource Area 4 for a typical winter season.

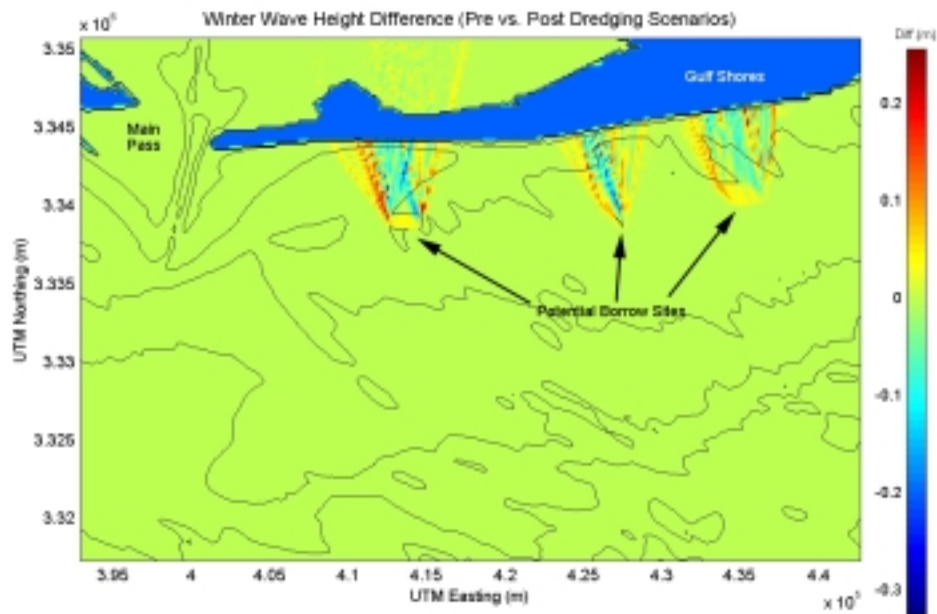


Figure B4-2. Wave height modifications caused by the offshore sand mining at Resource Areas 1, 2, and 3 for a typical winter season.

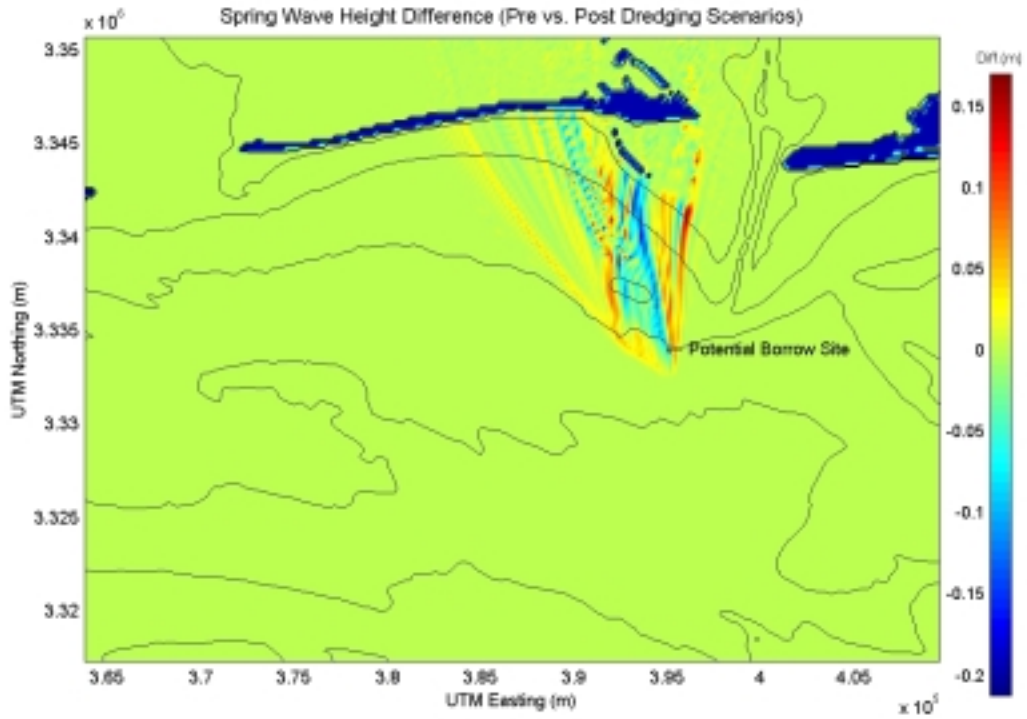


Figure B4-3. Wave height modifications caused by the offshore sand mining at Resource Area 4 for a typical spring season.

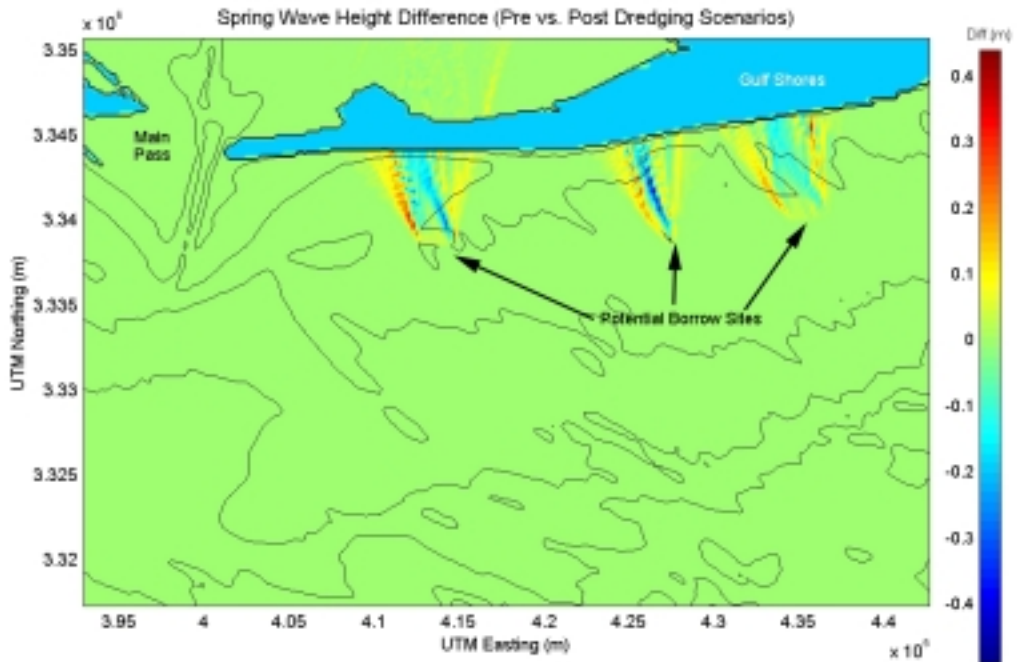


Figure B4-4. Wave height modifications caused by the offshore sand mining at Resource Areas 1, 2, and 3 for a typical spring season.

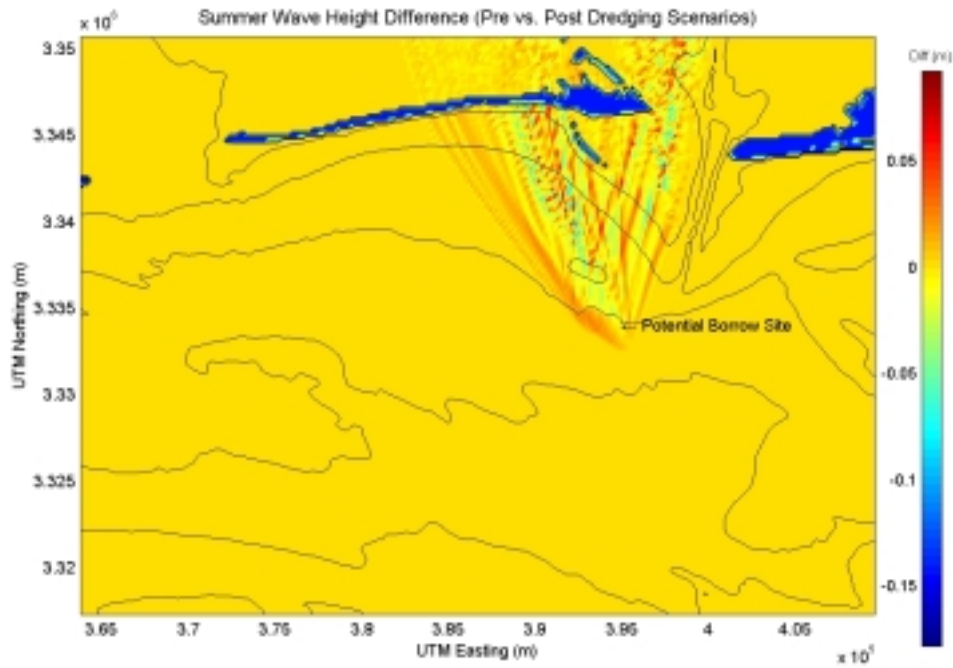


Figure B4-5. Wave height modifications caused by the offshore sand mining at Resource Area 4 for a typical summer season.

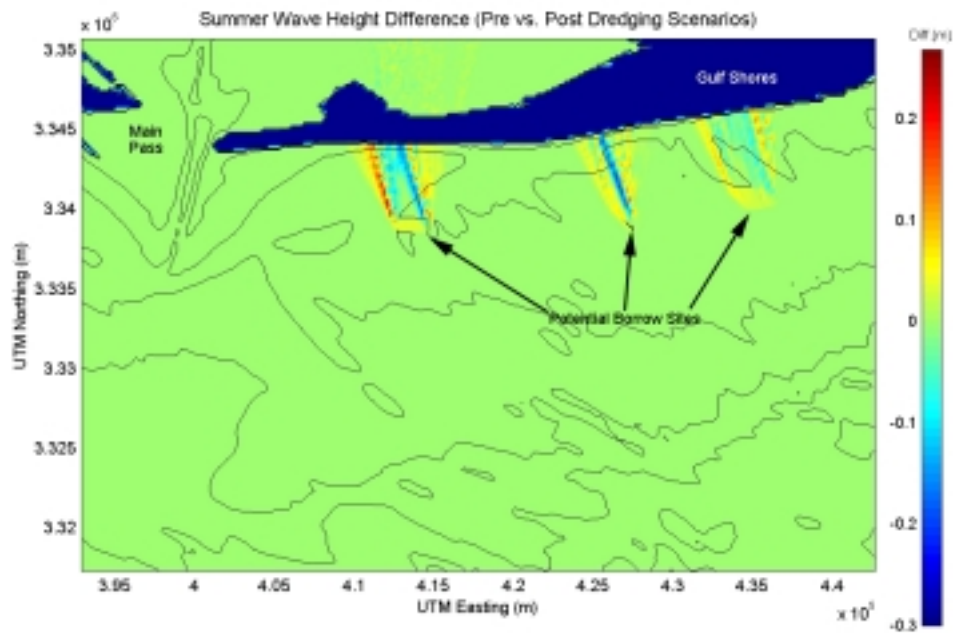


Figure B4-6. Wave height modifications caused by the offshore sand mining at Resource Areas 1, 2, and 3 for a typical summer season.

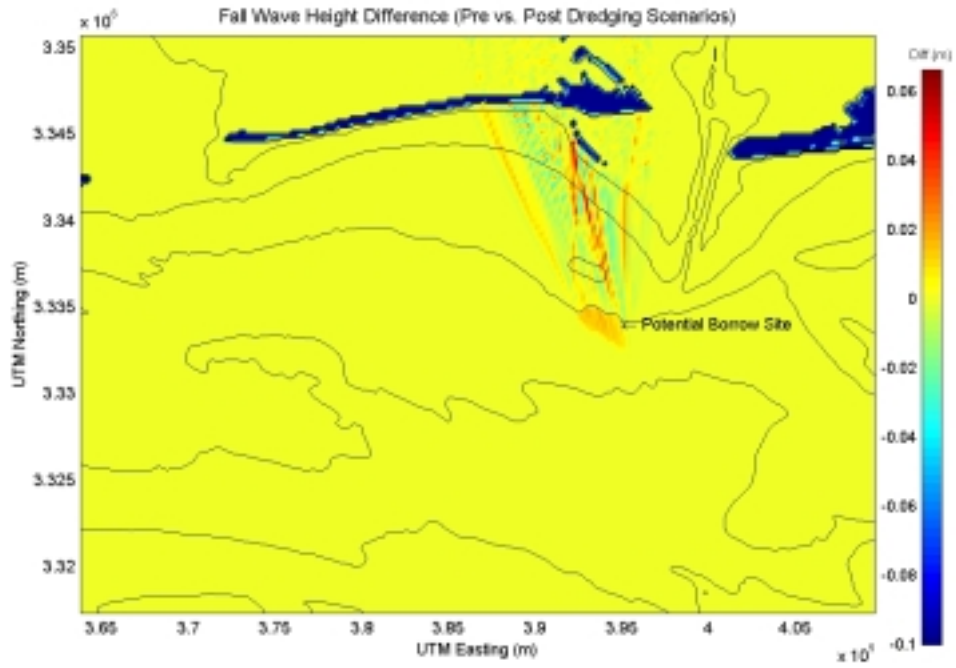


Figure B4-7. Wave height modifications caused by the offshore sand mining at Resource Area 4 for a typical fall season.

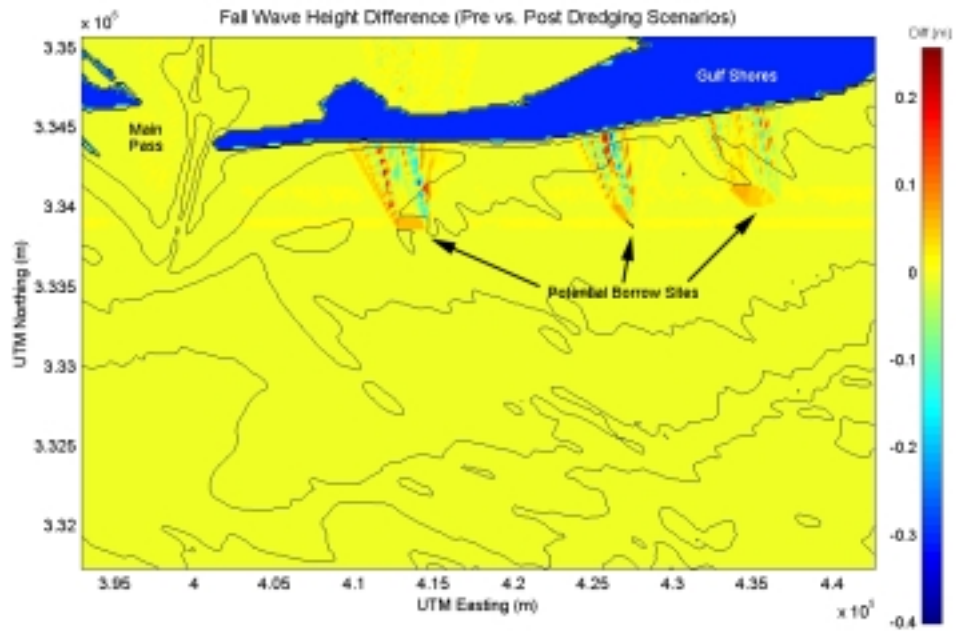


Figure B4-8. Wave height modifications caused by the offshore sand mining at Resource Areas 1, 2, and 3 for a typical fall season.

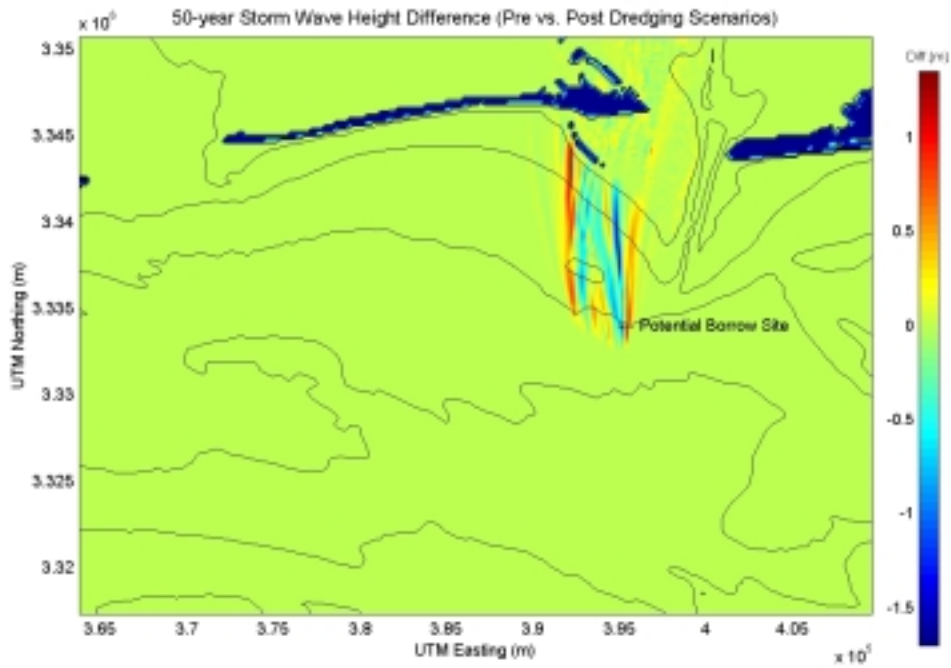


Figure B4-9. Wave height modifications caused by the offshore sand mining at Resource Area 4 for a 50-year storm.

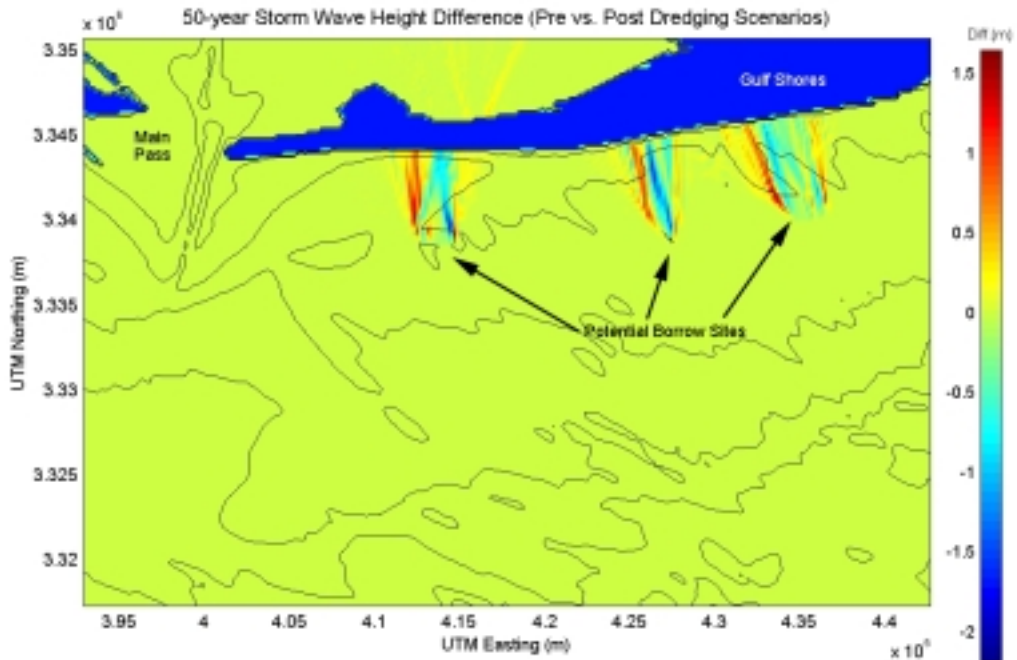


Figure B4-10. Wave height modifications caused by the offshore sand mining at Resource Areas 1, 2, and 3 for a 50-year storm.